Mean-field behavior in coupled oscillators with attractive and repulsive interactions

Hyunsuk Hong and Steven H. Strogatz

Phys. Rev. E **85**, 056210 — Published 23 May 2012

DOI: 10.1103/PhysRevE.85.056210

Mean-field behavior in coupled oscillators with attractive and repulsive interactions

Hyunsuk Hong[1] and Steven H. Strogatz[2]

[1]*Department of Physics and Research Institute of Physics and Chemistry, Chonbuk National University, Jeonju 561-756, Korea*

[2]*Department of Mathematics, Cornell University, NY 14853, U.S.A*

We consider a variant of the Kuramoto model of coupled oscillators in which both attractive and repulsive pairwise interactions are allowed. The sign of the coupling is assumed to be a characteristic of a given oscillator. Specifically, some oscillators repel all the others, thus favoring an antiphase relationship with them. Other oscillators attract all the others, thus favoring an in-phase relationship. The Ott-Antonsen ansatz is used to derive the exact low-dimensional dynamics governing the system's long-term macroscopic behavior. The resulting analytical predictions agree with simulations of the full system. We explore the effects of changing various parameters, such as the width of the distribution of natural frequencies and the relative strengths and proportions of the positive and negative interactions. For the particular model studied here, we find, unexpectedly, that the mixed interactions produce no new effects. The system exhibits conventional mean-field behavior, and displays a second-order phase transition like that found in the original Kuramoto model. In contrast to our recent study of a different model with mixed interactions [H. Hong and S. H. Strogatz, Phys. Rev. Lett. **106**, 054102 (2011)],the π-state and traveling wave state do not appear for the coupling type considered here.

PACS numbers: 05.45.Xt, 89.75.-k

I. INTRODUCTION

The Kuramoto model [1] has been used to shed light on the dynamics of a wide range of physical, chemical and biological systems, such as Josephson junction arrays [2], charge-density waves [3], laser arrays [4], collective atomic recoil lasers [5], bubbly fluids [6], neutrino flavor oscillations [7], electrochemical oscillators [8], and human crowd behavior [9].

One of the key assumptions in the Kuramoto model is that the mutual coupling between any two oscillators is positive. Positive coupling tends to pull the phases of the oscillators together, thus favoring synchrony. Negative coupling, on the other hand, pushes the phases apart and thus favors a phase difference of π. When both types of coupling are present, the system can become frustrated. In this case not much is known about what sorts of dynamics and equilibrium states might arise.

Even the mean-field version of such systems remains mysterious. Twenty years ago, Daido found evidence that Kuramoto models with mixed positive and negative coupling could undergo a glass transition [10], but the existence and properties of such an "oscillator glass" remain unclear [11]. Other models with mixed attractive/repulsive interactions have since been explored by several authors, who were also motivated by analogies to spin glasses, as well as to neural networks with mixed excitatory and inhibitory connections [12]. In each instance it has been difficult to understand the behavior of these models because of their inherent nonlinearity, quenched random interactions, and large numbers of degrees of freedom.

We wondered whether Daido's oscillator glass transition might be illuminated by studying much simpler models with mixed coupling. In this paper we analyze the behavior of one such model and find, unfortunately, that this particular simplification does not exhibit an oscillator glass. In fact, it doesn't do anything that hasn't already been seen in the traditional Kuramoto model where all the couplings are positive.

The model we examine is a set of N coupled oscillators:

$$\frac{d\phi_i}{dt} = \omega_i + \frac{1}{N}\sum_{j=1}^{N} K_j \sin(\phi_j - \phi_i), \quad i = 1, \cdots, N, \quad (1)$$

where ϕ_i is the phase of the ith oscillator, and ω_i is its intrinsic frequency, chosen at random from a prescribed probability density $g(\omega)$. We restrict attention from now on to the case of a Lorentzian distribution, $g(\omega) = \frac{1}{\pi}\frac{\gamma}{\omega^2+\gamma^2}$, with width γ and zero mean ($\langle\omega\rangle = 0$), for convenience.

The parameter K_j, which can be either positive or negative, encodes the strength and sign of the influence of oscillator j on all the other oscillators, including oscillator i. Note that this coupling parameter is oscillator-dependent, and in general would vary from one oscillator to another: $K_i \neq K_j$. Hence the pairwise interaction between two oscillators is typically non-symmetric. For the sake of analytical tractability, we consider the simplest non-trivial distribution of the interaction strength: $\Gamma(K) = (1-p)\delta(K-K_1) + p\delta(K-K_2)$, where $K_1 < 0$ and $K_2 > 0$ represent the intensity of the repulsive and attractive interactions, respectively, and p denotes the proportion of the oscillator population whose coupling strength is positive.

In a previous study [13], we considered a related but qualitatively different model with mixed interactions. The crucial difference was that in the earlier model, the oscillator-dependent coupling parameter was K_i, appearing *outside* the sum in the governing equation. Here it

is K_j, appearing *inside* the sum. This makes a world of difference, as we will see. In particular, the states we called the "π-state" and the "traveling wave state" [13] no longer appear.

To gain some intuition about the difference between the model considered in ref. [13] and the model considered in this paper, it helps to think of the oscillators and their interactions in human terms. Imagine that the oscillators "speak" and "listen" to one another when they interact. Then, in this metaphor, the oscillators of the previous model can be characterized by their *listening* styles. A "conformist" oscillator listens to the other oscillators and tries to align its phase to each of theirs, whereas a "contrarian" oscillator prefers a phase difference of π with everyone else.

In the present model, by contrast, the oscillators are characterized by their *speaking* styles. Attractive oscillators send signals that draw other oscillators toward them, thus favoring zero phase difference. Repulsive oscillators drive others as far away from themselves as possible (namely, toward a phase difference of π).

We are mainly interested in exploring such systems of oscillators for theoretical reasons, as mentioned above, but there are some real-world examples of physical, biological, and chemical systems where similar phenomena arise. For example, many neurons obey Dale's principle, which states that a neuron "speaks" in the same way at all of its synaptic connections to other cells, in the sense that it releases the same set of neurotransmitters at all of its synapses [14]. Our model Eq. (1) embodies an idealized version of this assumption by postulating that each oscillator j influences all the others with the same coupling strength and sign, as quantified by the parameter K_j. Likewise, our previous model has been shown by Montbrio and Pazó [15] to be relevant to arrays of nanomechanical oscillators [16] and ion chains interacting via Coulomb forces [17].

In what follows we will be particularly interested in how varying p, the proportion of the system consisting of attractive oscillators, affects the synchronization behavior of Eq. (1). We analyze the system using the Ott-Antonsen ansatz [18] as well as the traditional self-consistency equation for the order parameter [1].

II. DIMENSIONAL REDUCTION BY OTT-ANTONSEN THEORY

Collective synchronization has been conveniently described by the complex order parameter defined by [1]:

$$Z(t) \equiv Re^{i\theta} = \frac{1}{N}\sum_{j=1}^{N} e^{i\phi_j}, \tag{2}$$

where the magnitude R measures the phase coherence, and θ the average phase. Another order parameter we consider here is given by

$$W(t) \equiv Se^{i\Phi} = \frac{1}{N}\sum_{j=1}^{N} K_j e^{i\phi_j}, \tag{3}$$

which is a sort of "*weighted*" mean field. We investigate the synchronization behavior as the ratio of the attractive and repulsive interaction strength $Q \equiv -K_1/K_2 > 0$ is varied. For convenience, we set $K_2 = 1$ (which can be achieved without loss of generality by rescaling time), and vary the value of K_1. Three different regimes of Q are considered: $Q < 1$, $Q = 1$, and $Q > 1$.

We begin with our analytical results. In the continuum limit $N \to \infty$, Eq. (1) gives rise to a continuity equation for the probability density function $f(\phi, K, \omega, t)$:

$$\frac{\partial f}{\partial t} + \frac{\partial}{\partial \phi}(fv) = 0, \tag{4}$$

where $v = v(\phi, \omega, t)$ is the velocity function given by

$$v = \omega + \int\int\int K \sin(\phi' - \phi) f(\phi', K, \omega, t) d\phi' \Gamma(K) dK d\omega. \tag{5}$$

Following the approach introduced by Ott and Antonsen [18], we consider the family of special density functions f given by Poisson kernels:

$$f(\phi, K, \omega, t) = \frac{g(\omega)}{2\pi}\left\{1 + \left[\sum_{n=1}^{\infty}[a(K,\omega,t)]^n e^{in\phi} + \text{c.c.}\right]\right\}, \tag{6}$$

where c.c. denotes the complex conjugate. In the continuum limit, the order parameter $W(t)$ is given by

$$W(t) = \int\int\int K e^{i\phi'} f(\phi', K, \omega, t) d\phi' \Gamma(K) dK d\omega. \tag{7}$$

Using Eq. (7), the velocity function v simplifies to

$$v = \omega + \frac{1}{2i}(We^{-i\phi} - \overline{W}e^{i\phi}), \tag{8}$$

where the overbar indicates complex conjugation. Substituting Eq. (8) and (6) into Eq. (4), we find a satisfies the equation

$$\dot{a} = -i\omega a + \frac{1}{2}(\overline{W} - Wa^2), \tag{9}$$

where W becomes

$$W(t) = \int\int K \bar{a}(K, \omega, t) g(\omega) d\omega \Gamma(K) dK \tag{10}$$

since only $n = 1$ in the c.c. term of f in Eq. (6) contributes to the ϕ-integral. We do the contour integral with respect to ω, and close the contour in the lower half plane in ω-space. Equation (10) is then given by

$$W(t) = \int K \bar{a}(K, -i\gamma, t) \Gamma(K) dK. \tag{11}$$

If we let $z(K,t) \equiv a(K,-i\gamma,t)$, $z(K,t)$ is satisfied with

$$\dot{z} = -\gamma z + \frac{1}{2}(\overline{W} - W z^2) \tag{12}$$

according to Eq. (9). Using the distribution $\Gamma(K) = (1-p)\delta(K-K_1)+p\delta(K-K_2)$, we find $W(t)$ is rewritten as

$$W(t) = (1-p)K_1\bar{z}_1 + pK_2\bar{z}_2, \tag{13}$$

where $z_1 = z(K_1,t)$ and $z_2 = z(K_2,t)$, respectively. We then find the dynamics of z_1 and z_2 is given by

$$\begin{aligned}\dot{z}_1 &= -\gamma z_1 + \tfrac{1}{2}[qK_1 z_1 + pK_2 z_2 - (qK_1\bar{z}_1 + pK_2\bar{z}_2)z_1^2],\\ \dot{z}_2 &= -\gamma z_2 + \tfrac{1}{2}[qK_1 z_1 + pK_2 z_2 - (qK_1\bar{z}_1 + pK_2\bar{z}_2)z_2^2]\end{aligned} \tag{14}$$

according to Eq. (12), where $q = 1-p$. Introducing $Q \equiv -K_1/K_2$, rescaling the time by $K_2 t/2$, and redefining γ/K_2 by γ in the rescaled time, Eq. (14) becomes

$$\begin{aligned}\dot{z}_1 &= -2\gamma z_1 - [(qQz_1 - pz_2) - (qQ\bar{z}_1 - p\bar{z}_2)z_1^2],\\ \dot{z}_2 &= -2\gamma z_2 - [(qQz_1 - pz_2) - (qQ\bar{z}_1 - p\bar{z}_2)z_2^2].\end{aligned} \tag{15}$$

With the expression $z_1 = r_1 e^{-i\theta_1}$ and $z_2 = r_2 e^{-i\theta_2}$, Eq. (15) is given by

$$\begin{aligned}\dot{r}_1 &= -2\gamma r_1 - (1-r_1^2)(qQr_1 - pr_2\cos\delta),\\ \dot{r}_2 &= -2\gamma r_2 - (1-r_2^2)(qQr_1\cos\delta - pr_2),\\ \dot{\delta} &= \sin\delta\left[qQ\tfrac{r_1}{r_2}(1+r_2^2) - p\tfrac{r_2}{r_1}(1+r_1^2)\right],\end{aligned} \tag{16}$$

where $r_{1,2} \neq 0$ and $\delta \equiv \theta_1 - \theta_2$. The upshot is that, when restricted to the family of Poisson kernel densities, the dynamics of the original high-dimensional system governed by Eq. (1) reduces exactly to the three-dimensional dynamical system for (r_1, r_2, δ) given by Eq. (16).

The order parameter $Z(t)$ also simplifies:

$$\begin{aligned}Z &= \int\int\int e^{i\phi} f(\phi,K,\omega,t)d\phi\Gamma(K)dKd\omega\\ &= \int\int \bar{a}(K,\omega,t)g(\omega)d\omega\Gamma(K)dK\\ &= \int \bar{a}(K,-i\gamma,t)\Gamma(K)dK\\ &= \int \bar{z}(K,t)\Gamma(K)dK,\end{aligned} \tag{17}$$

which finally yields

$$Z(t) = (1-p)\bar{z}_1 + p\bar{z}_2. \tag{18}$$

With the dynamics of z_1 and z_2 in Eq. (15), we can find the dynamics of the order parameters $W(t)$ and $Z(t)$ shown in Eq. (13) and (18).

III. FIXED POINT ANALYSIS

We next examine the fixed point solution with $\dot{z}_1 = 0$ and $\dot{z}_2 = 0$. From Eq. (12) we find

$$\begin{aligned}\dot{z}_1 &= -\gamma z_1 + \tfrac{1}{2}(\overline{W} - W z_1^2),\\ \dot{z}_2 &= -\gamma z_2 + \tfrac{1}{2}(\overline{W} - W z_2^2).\end{aligned} \tag{19}$$

For $\dot{z}_1 = 0$ and $\dot{z}_2 = 0$, Eq. (19) is given by

$$\begin{aligned}z_1 &= \frac{1}{2\gamma}(\overline{W} - W z_1^2),\\ z_2 &= \frac{1}{2\gamma}(\overline{W} - W z_2^2).\end{aligned} \tag{20}$$

Using $W = -qQ\bar{z}_1 + p\bar{z}_2$, we find

$$p = \frac{W + Q\bar{z}_1}{Q\bar{z}_1 + \bar{z}_2}. \tag{21}$$

Assuming W is real and positive (which entails no loss of generality, since we can rotate coordinates), and noting that $W(t)$ is constant, by the fixed point assumption, we then find

$$p = \bar{p} = \frac{\overline{W} + Qz_1}{Qz_1 + z_2}. \tag{22}$$

Then, $\overline{W} = S$ and we have

$$\begin{aligned}z_1 &= \tfrac{1}{2\gamma}(S - Sz_1^2),\\ z_2 &= \tfrac{1}{2\gamma}(S - Sz_2^2),\\ p &= \tfrac{S+Qz_1}{Qz_1+z_2}.\end{aligned} \tag{23}$$

Solving for z_1 and z_2, we find

$$z_1 = z_2 = \frac{-\gamma + \sqrt{\gamma^2 + S^2}}{S}, \tag{24}$$

and substituting Eq. (24) into Eq. (23), we find that p is given by

$$p = \frac{1}{1+Q}\left[\frac{S^2}{-\gamma + \sqrt{\gamma^2+S^2}} + Q\right]. \tag{25}$$

Note that Eq. (24) corresponds to the $\delta = 0$ state.

We now analyze the linear stability of the incoherent state $Z = W = 0$. Since $|z_1| \ll 1$ and $|z_2| \ll 1$ in the incoherent state, the linearized system is given by

$$\dot{z}_1 = -2\gamma z_1 + (-qQz_1 + pz_2) \tag{26}$$

$$\dot{z}_2 = -2\gamma z_2 + (-qQz_1 + pz_2) \tag{27}$$

from Eq. (15), ignoring the higher order terms. Multiplying Eq. (26) by $-qQ$ and Eq. (27) by p, and adding the two equations, we obtain

$$\begin{aligned}\dot{\overline{W}} &= -2\gamma\overline{W} + (p - qQ)\overline{W},\\ &= (-2\gamma + \langle K\rangle)\overline{W},\end{aligned} \tag{28}$$

where we used $\langle K\rangle = p - qQ$, recalling $W = -qQ\bar{z}_1 + p\bar{z}_2$ from Eq. (13) with $Q = -K_1/K_2$ and $K_2 = 1$. We then find that $\overline{W}$ goes to zero exponentially fast if $\langle K\rangle < 2\gamma$, but it does not if $\langle K\rangle > 2\gamma$. Therefore, from this we conclude that the incoherent state ($Z = W = 0$) is stable for $p < p^\star$, where

$$p^\star = \frac{2\gamma + Q}{1 + Q}. \tag{29}$$

This critical value $p^\star$ can also be obtained from Eq. (25) by looking at the limit as S goes to zero. Curiously, the same value for $p^\star$ arose in our previous study [13] where the coupling strength K_i was outside the summation.

IV. SELF-CONSISTENCY EQUATION FOR THE ORDER PARAMETER

Alternatively, we can deduce $p^\star$ by the usual self-consistency argument. Substituting the order parameter W into Eq. (1), we find that the governing equation becomes

$$\dot{\phi}_i = \omega_i - S\sin(\phi_i - \Phi). \tag{30}$$

When the effective coupling S is large enough to overcome the diversity of the natural frequencies (i.e., when $S > |\omega_i|$), Eq. (30) exhibits a phase-locked solution with $\dot{\phi}_i = 0$:

$$\phi_i = \Phi + \sin^{-1}(\omega_i/S). \tag{31}$$

On the other hand, when the natural frequency is too highly detuned relative to S, i.e., for $|\omega_i| > S$, Eq. (30) shows a drifting solution with $\phi_i(t) \simeq \phi_i(0) + \omega_i t$. The self-consistency equation for S is then given by

$$\begin{aligned} Se^{i\Phi} &= \int_{-\pi}^{\pi}\int_{-S}^{S} Ke^{i[\Phi+\sin^{-1}(\frac{\omega}{S})]}\Gamma(K)dKg(\omega)d\omega \\ &= e^{i\Phi}\langle K\rangle\int_{-S}^{S}\sqrt{1-(\omega/S)^2}g(\omega)d\omega, \end{aligned} \tag{32}$$

where the contribution from the drifting solution is canceled out due to the symmetry of $g(\omega)$. With the Taylor expansion of $g(\omega)$, we find that Eq. (32) is given by

$$S = \frac{\pi}{2}g(0)\langle K\rangle S + \frac{\pi}{16}g''(0)\langle K\rangle S^3 + \mathcal{O}(S^5), \tag{33}$$

which yields

$$S \sim (p - p_c)^{1/2} \tag{34}$$

with

$$p_c = \frac{2\gamma + Q}{1 + Q}. \tag{35}$$

This p_c is obtained from the condition

$$\frac{\pi}{2}g(0)\langle K\rangle = 1. \tag{36}$$

Note that this p_c is consistent with the value $p^\star$ in Eq. (29). This implies that the incoherent state is stable for $p < p_c$, and the synchronization transition from the incoherent state to the coherent one occurs at p_c. The order parameter R is linearly proportional to S for small values of S, so R is also characterized by

$$R \sim (p - p_c)^{1/2} \tag{37}$$

with the same p_c as Eq. (35). This mean-field behavior was predicted previously by Paissan and Zanette [19].

V. NUMERICAL RESULTS

We now numerically examine the predicted steady-state values of z_1 and z_2 according to Eq. (15). Using those z_1 and z_2, we obtain W and Z given by Eq. (13) and (18). The values of W and Z obtained in this way are shown as the red solid line and the blue dashed line in Fig. 1.

For comparison, we can also numerically integrate the full system governed by Eq. (1), and measure $W(t)$ and $Z(t)$ according to Eq. (2) and (3). Integrations of Eq. (1) were performed using Heun's method [20] with a discrete time step $\delta t = 0.01$. For the total $N_t = 5 \times 10^4$ time steps, the equation of motion was integrated. The initial 3×10^3 steps were discarded as a transient.

For the sake of illustration, let us fix the width of the frequency distribution at $\gamma = 0.05$. The open pink and filled sky blue boxes in Fig. 1 show the simulation results obtained for the full system. The analytical predictions based on the reduced system are in good agreement with the simulations. In particular, the synchronization transition from $R = 0$ to $R \neq 0$ is found to occur at $p \simeq 0.4$, as predicted theoretically.

Figure 2 shows R and S as a function of p for various values of Q and γ. We find that the critical value p_c is increased when either the width γ or the interaction ratio Q are increased. These trends make sense; increasing the width of $g(\omega)$ or increasing the strength of repulsive interactions both make the system harder to synchronize.

Incidentally, the behavior of S shown in the right panels of Fig. 1 looks like a linear dependence on p. But it is not. Closer examination, both numerically and analytically, reveals the standard mean-field behavior with an order parameter exponent $\beta = 1/2$.

We were surprised to find that different values of Q did not yield qualitatively different behavior, unlike what we found in our previous study [13]. In particular, the mean phase velocity in the present model always equals the mean of the oscillators' intrinsic frequencies. Thus the traveling wave state found in Ref. [13] does not appear in the present system.

Nor did we see any evidence of the $\delta = \pi$ state found in our previous study [13]. To look for it, we examined two different subpopulations in the phase distribution function: one is the subpopulation of oscillators with attractive interactions ($K_2 > 0$) and the other is the subpopu-

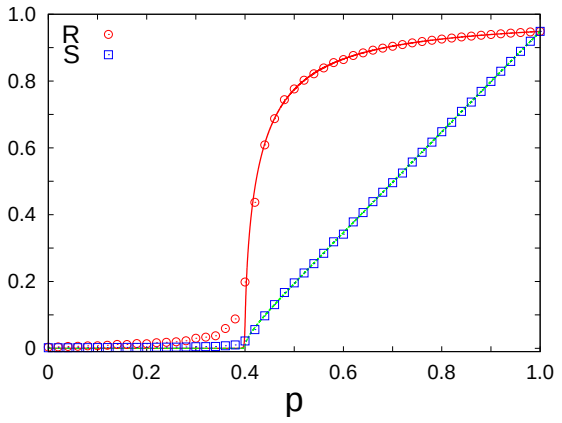

FIG. 1: (Color online) Behavior of the order parameters R and S vs. p, the fraction of the system with positive coupling, for $\gamma = 0.05$ and $Q = 0.5$. The red solid line and the green dashed line represent the theoretical predictions of R and S, respectively. The red circles and the blue boxes denote simulation results for R and S, respectively, obtained by integrating the full system Eq. (1). System size: $N = 12800$ oscillators. The data shown were obtained by averaging over 10 samples.

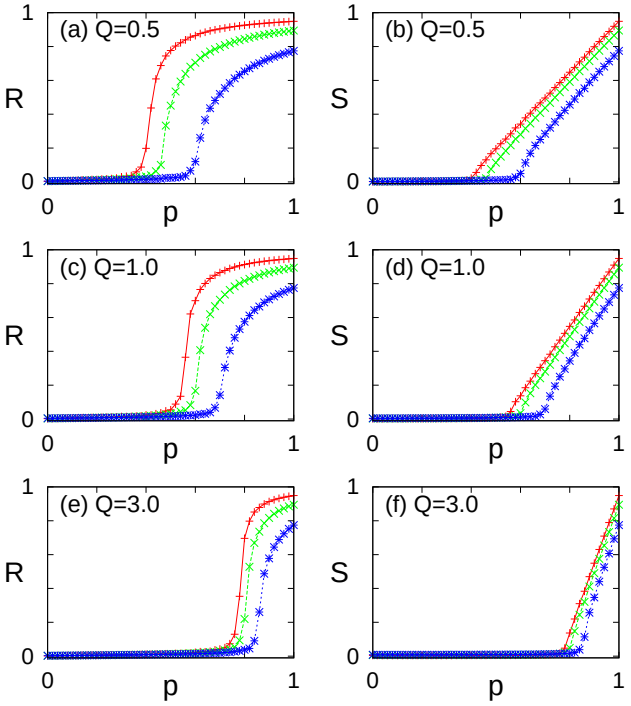

FIG. 2: (Color online) Behavior of the order parameters R (left panels) and S (right panels) as a function of p, varying the values of Q and γ. Symbols: red plus-signs for $\gamma = 0.05$; green diagonal crosses for $\gamma = 0.1$; blue asterisks for $\gamma = 0.2$. System size: $N = 12800$. Numerical data obtained by averaging over 10 samples.

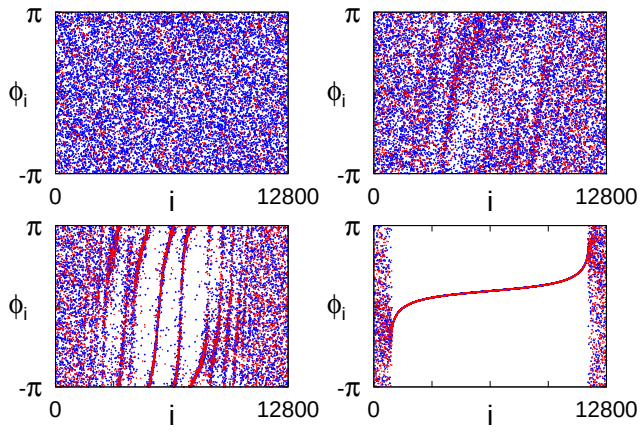

FIG. 3: (Color online) The phase ϕ_i of the ith oscillator is plotted as a function of the oscillator index i for various values of p. Top left panel, $p = 0.2(< p_c)$; top right panel, $p = 0.3(< p_c)$; bottom left panel, $p = 0.4(= p_c)$; bottom right panel, $p = 0.5(> p_c)$. The system size is $N = 12800$, and $\gamma = 0.05$ and $Q = 0.5$. The red plus-signs represent the phases of the oscillators with attractive interaction, $K_2 > 0$. Blue diagonal crosses denote the phases of the oscillators with repulsive interactions, $K_1 < 0$.

lation of oscillators with repulsive interactions ($K_1 < 0$). Figure 3 displays the phases of the oscillators in each subpopulation. We find that the phases of the oscillators in each subpopulation show a fully random distribution for $p < p_c$, but they show the same value for $p > p_c$, implying a $\delta = 0$ state instead of a $\delta = \pi$ state, thus yielding another difference from our previous study [13].

To explain intuitively why the previous and current models behave so differently, recall that the dynamics of the model in [13] were governed by $\dot{\phi}_i = \omega_i - K_i R \sin(\phi_i - \Theta)$. Therefore *two* kinds of phase-locked state are possible, depending on the sign of K_i. The oscillators with attractive coupling $K_2 > 0$ obey $\dot{\phi}_i = \omega_i - K_2 R \sin(\phi_i - \Theta)$ whereas those with repulsive coupling $K_1 < 0$ obey $\dot{\phi}_i = \omega_i + |K_1| R \sin(\phi_i - \Theta)$. The two stable fixed points of these equations together form the π-state, in which two groups of oscillators are aligned in antiphase: $\delta = \pi$. Furthermore, they may induce a mismatch between the mean phase velocities of the two groups, which yields the traveling wave state.

On the other hand, the present system shows only *one* phase-locked state given by Eq. (30), so the traveling wave state as well as the π-state does not exist.

Acknowledgments

H.H acknowledges the hospitality of Cornell University during the visit for sabbatical leave. S.H.S acknowledges the support by NSF Grants CCF-0835706 and CCF-0832782. We thank the Korea Institute for Advanced

Study for providing computing resources for the project.

[1] Y. Kuramoto, *Chemical Oscillations, Waves and Turbulence* (Springer, New York, 1984).

[2] J. W. Swift, S. H. Strogatz, and K. Wiesenfeld, Physica D **55**, 239 (1992); K. Wiesenfeld, Physica B **222**, 315 (1996); K. Wiesenfeld, P. Colet, and S. H. Strogatz, Phys. Rev. Lett. **76**, 404 (1996); *ibid.*, Phys. Rev. E **57**, 1563 (1998); K. Park and M. Y. Choi, Phys. Rev. B **56**, 387 (1997); G. Filatrella, N. F. Pedersen, and K. Wiesenfeld, Phys. Rev. E **61**, 2513 (2000); B. C. Daniels, S. T. M. Dissanayake, and B. R. Trees, Phys. Rev. E **67**, 026216 (2003).

[3] G. Grüner and A. Zettl, Phys. Rep. **119**, 117 (1985); G. Grüner, Rev. Mod. Phys. **60**, 1129 (1988); S. H. Strogatz and R. E. Mirollo, J. Phys. A **21**, L699 (1988); *ibid.*, Physica D **31**, 143 (1989); C. M. Marcus, S. H. Strogatz, and R. M. Westervelt, Phys. Rev. B **40**, 5588 (1989).

[4] Y. Braiman, T. A. B. Kennedy, K. Wiesenfeld, and A. Khibnik, Phys. Rev. A **52**, 1500 (1995); S. Yu. Kourtchatov, V. V. Likhanskii, A. P. Napartovich, F. T. Arecchi, and A. Lapucci, Phys. Rev. A **52**, 4089 (1995); G. Kozyreff, A. G. Vladimirov, and P. Mandel, Phys. Rev. Lett. **85**, 3809 (2000); *ibid.*, Phys. Rev. E **64**, 016613 (2001); R. A. Oliva and S. H. Strogatz, Int. J. Bifurcation Chaos **11**, 2359 (2001); A. G. Vladimirov, G. Kozyreff, and P. Mandel, Europhys. Lett. **61**, 613 (2003).

[5] C. von Cube *et al.*, Phys. Rev. Lett. **93**, 083601 (2004); J. Javaloyes, M. Perrin, A. Politi, Phys. Rev. E **78**, 011108 (2008).

[6] G. Russo and P. Smereka, SIAM. J. Appl. Math. **56**, 327 (1996).

[7] J. Pantaleone, Phys. Rev. D **58**, 073002 (1998).

[8] N. Mazouz, K. Krischer, G. Flätgen, and G. Ertl, J. Phys. Chem. B **101**, 2403 (1997); I. Z. Kiss, W. Wang, and J. L. Hudson, Chaos **12**, 252 (2002); M. Wickramasinghe and I. Z. Kiss, Phys. Rev. E **83**, 016210 (2011).

[9] Z. Néda, E. Ravasz, Y. Brechet, T. Vicsek, and A.-L. Barabási, Nature **403**, 849 (2000); Z. Néda, E. Ravasz, T. Vicsek, Y. Brechet, and A.-L. Barabási, Phys. Rev. E **61**, 6987 (2000).

[10] H. Daido, Phys. Rev. Lett. **68**, 1073 (1992).

[11] H. Daido, Phys. Rev. E **61**, 2145 (2000); J. C. Stiller and G. Radons, Phys. Rev. E **58**, 1789 (1998).

[12] H. Daido, Prog. Theor. Phys. **77**, 622 (1987); L. L. Bonilla, C. J. P. Vicente, and J. M. Rubi, J. Stat. Phys. **70**, 921 (1993); D. H. Zanette, Europhys. Lett. **72**, 190 (2005).

[13] H. Hong and S. H. Strogatz, Phys. Rev. Lett. **106**, 054102 (2011).

[14] J. C. Eccles, Notes Rec. R. Soc. Lond. **30**, 219 (1976).

[15] E. Montbrio and D. Pazó, Phys. Rev. Lett. **106**, 254101 (2011).

[16] M. C. Cross, A. Zumdieck, R. Lifshitz, and J. L. Rogers, Phys. Rev. Lett. **93**, 224101 (2004); M. C. Cross, J. L. Rogers, R. Lifshitz, and A. Zumdieck, Phys. Rev. E **73**, 036205 (2006); S. -B. Shim, M. Imboden, and P. Mohanty, Science **316**, 95 (2007).

[17] T. E. Lee and M. C. Cross, Phys. Rev. Lett. **106**, 143001 (2011).

[18] E. Ott and T. M. Antonsen, Chaos **18**, 037113 (2008); E. Ott and T. M. Antonsen, Chaos **19**, 023117 (2009).

[19] G. H. Paissan and D. H. Zanette, Physica D **237**, 818 (2008).

[20] See, e.g., R.L. Burden and J.D. Faires, *Numerical Analysis* (Brooks/Cole, Pacific Grove, 1997), p.280.